

Received September 15, 2020, accepted September 28, 2020, date of publication October 5, 2020, date of current version October 15, 2020.

Digital Object Identifier 10.1109/ACCESS.2020.3028698

# Electromechanical Equivalent Circuit Model of a Piezoelectric Disk Considering Three Internal Losses

XIAOXIAO DONG<sup>1</sup>, (Member, IEEE), KENJI UCHINO<sup>2</sup>, (Life Fellow, IEEE),  
CHUNRONG JIANG<sup>3</sup>, LONG JIN<sup>4</sup>, ZHIKE XU<sup>4</sup>, AND YUE YUAN<sup>1</sup>, (Member, IEEE)

<sup>1</sup>College of Energy and Electrical Engineering, Hohai University, Nanjing 211100, China

<sup>2</sup>International Center for Actuators and Transducers, The Pennsylvania State University, University Park, PA 16802, USA

<sup>3</sup>College of Electric Power Engineering, Nanjing Institute of Technology, Nanjing 211167, China

<sup>4</sup>College of Electrical Engineering, Southeast University, Nanjing 210098, China

Corresponding author: Xiaoxiao Dong (dongxiaoxiao@hhu.edu.cn)

This work was supported in part by the Fundamental Research Funds for the Central Universities under Grant 2018B06914, and in part by the National Natural Science Foundation of China under Grant 51777029.

**ABSTRACT** Heat generation by internal loss factors of piezoelectrics is one of the critical issues for high power density piezoelectric applications, such as ultrasonic motors, piezoelectric actuators and transducers. There are three types of internal losses in piezoelectric materials, namely dielectric, elastic and piezoelectric losses. In this paper, a decoupled equivalent circuit is proposed to emulate a piezoelectric disk in radial vibration mode considering all three types of internal losses. First, the decoupled equivalent circuit is derived according to the conventional electromechanical equivalent circuit model. Then, a piezoelectric disk configuration in radial vibration mode is explored and simulated. The resonance and antiresonance frequencies and their corresponding mechanical quality factors are achieved by the proposed circuit. In order to verify the accuracy of the simulation results, the piezoelectric disk is fabricated and tested. Simulation results with the new circuit exhibit a good agreement with experimental results. Finally, the equivalent circuit with only dielectric and elastic losses are simulated and compared which further validates the accuracy improvement of the new equivalent circuit considering all three losses.

**INDEX TERMS** Piezoelectric material, equivalent circuit, radial vibration, loss factor, piezoelectric loss.

## I. INTRODUCTION

Piezoelectric ultrasonic motors have developed rapidly since the 1980s, due to the superiority of high efficiency in the mm-size motor area [1]–[3]. The bottleneck of piezoelectric ultrasonic motors has been identified as heat generation, which is a significant problem for high power density applications [4]. Internal losses in piezoelectric materials are considered in general to have three different mechanisms, namely dielectric, mechanical, and piezoelectric losses [5]. Accurate determination of three types of losses is critical, since they are closely related to the heat generation mechanism in piezoelectrics.

Mechanical quality factors are basically related to the three types of losses and play a significant role in the study of heat generation of piezoelectric devices [6]. A higher mechanical

quality factor reduces the heat generation and increases the efficiency. Electromechanical equivalent circuit (EC) model is one of the most effective method to analyze the properties of piezoelectric vibrator [7]–[9]. IEEE Standard only provides a method to obtain the mechanical quality factor ( $Q_m$ ) at resonance frequency according to an EC model [10]. However, the main issue of this standard method is that it assumes piezoelectric loss to be the average value of elastic and dielectric losses, which results in the equivalence of  $Q$  values at resonance and antiresonance. This conclusion is proved to be inaccurate because experimental results indicate there exists a conspicuous discrepancy between the mechanical quality factors at the resonance ( $Q_R$ ) and the antiresonance ( $Q_A$ ) in lead-zirconate-titanate (PZT)-based ceramics [11]–[13]. In recent, the equivalent circuit of piezoelectrics for  $k_{31}$  vibration mode considering all three losses have been proposed by researchers at Pennsylvania State University [14], which explains the variation of the mechanical quality factor

The associate editor coordinating the review of this manuscript and approving it for publication was Hui Xie<sup>1</sup>.

between resonance and antiresonance frequencies. Further, a six-terminal EC of a ring-type piezoelectrics is proposed including three types of losses, which is utilized in characteristic analysis of an ultrasonic motor [15].

The piezoelectric disk of radial vibration mode is widely used as a vibrator for piezoelectric ultrasonic motors and transducers due to its large power density [16]. Although EC models of  $k_p$  vibration mode reported in existing literatures is efficient for analyzing the resonance and antiresonance frequencies [17]–[19], it is insufficient to achieve accurate mechanical quality factors without considering all three losses in piezoelectrics. In this paper, a decoupled EC of a piezoelectric disk in radial vibration mode is firstly derived considering all three types of internal losses. Based on the proposed electromechanical EC model, mechanical quality factors at resonance and antiresonance frequencies are calculated as a function of three types of losses. In addition, the relationship between frequencies and material properties of the piezoelectric disk is discussed to facilitate the designing of piezoelectric vibrators. Finally, the simulation results obtained from the EC model are compared with and verified by experimental results.

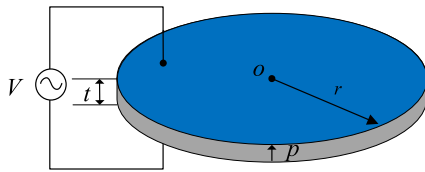


FIGURE 1. Schematic view of a piezoelectric disk.

## II. ELECTROMECHANICAL EQUIVALENT CIRCUIT OF A PIEZOELECTRIC DISK

### A. CONVENTIONAL EQUIVALENT CIRCUIT WITHOUT LOSSES

The configuration of a piezoelectric disk in radial vibration mode is shown in Figure 1. The piezoelectric ceramic thin disk is polarized in its thickness direction and the electrode areas are applied on its upper and lower surfaces. The radial vibration mode is excited by applying an AC voltage at the electrode areas. The conventional electromechanical EC of the piezoelectric disk is shown in Figure 2 [20].

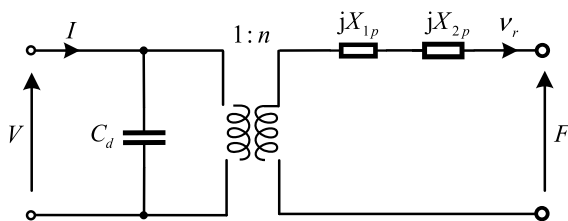


FIGURE 2. Conventional electromechanical equivalent circuit of the piezoelectric disk.

In Figure 2,  $V$  and  $I$  denote the input voltage and current in the electrical branch (i.e., the primary side of the equivalent

transformer), respectively.  $F$  is the output force and  $v_r$  is the vibration velocity in the mechanical branch (i.e., the secondary side of the equivalent transformer).  $C_d$  is the damped capacitance expressed as

$$C_d = \frac{S}{t} [\epsilon_{33}^T - \frac{2d_{31}^2}{s_{11}^E(1-\sigma)}] \quad (1)$$

in which  $\epsilon_{33}^T$  represents the absolute dielectric permittivity under constant stress; the Poisson's ratio  $\sigma$  is expressed by  $\sigma = -s_{12}^E/s_{11}^E$ ;  $s_{11}^E$  and  $s_{12}^E$  stand for the elastic compliance under constant electric field, and  $d_{31}$  denotes the piezoelectric constant; The area of the end of the piezoelectric disk can be described as  $S = \pi r^2$ ;  $r$  is the radius;  $t$  is the disk thickness.

The force factor  $n$  is the electromechanical conversion coefficient of the piezoelectric disk in radial vibration and expressed as

$$n = 2\pi r \cdot \frac{d_{31}}{s_{11}^E(1-\sigma)} \quad (2)$$

In the mechanical branch,  $X_{1p}$  and  $X_{2p}$  are impedances described as

$$X_{1p} = -\rho v_p S_r \frac{J_0(kr)}{J_1(kr)} \quad (3)$$

$$X_{2p} = \frac{\rho v_p S_r (1-\sigma)}{kr} \quad (4)$$

Here,  $\rho$  is the density;  $S_r$  is the area of the side of the piezoelectric disk expressed as  $S_r = 2\pi r t$ ;  $J_0$  and  $J_1$  are Bessel functions of the first kind; the wave number  $k$  is expressed by  $k = \omega/v_p$ ;  $\omega$  stands for the angular frequency;  $v_p$  represents the sound velocity and is expressed as

$$v_p = \sqrt{\frac{1}{\rho s_{11}^E} \cdot \frac{1}{1-\sigma^2}} \quad (5)$$

### B. EQUIVALENT CIRCUIT WITH THE INTEGRATION OF THREE TYPES OF LOSSES

The heat dissipation in the piezoelectric disk is generally originated from three types of loss factors: dielectric ( $\tan \delta'_{33}$ ), mechanical ( $\tan \phi'_{11}$ ,  $\tan \phi'_{12}$ ), and piezoelectric ( $\tan \theta'_{31}$ ) losses. Losses are integrated into the conventional electromechanical EC by complex parameters expressed as

$$\epsilon_{33}^T = \epsilon_{33}^T (1 - j \tan \delta'_{33}) \quad (6)$$

$$s_{11}^E = s_{11}^E (1 - j \tan \phi'_{11}) \quad (7)$$

$$s_{12}^E = s_{12}^E (1 - j \tan \phi'_{12}) \quad (8)$$

$$d_{31} = d_{31} (1 - j \tan \theta'_{31}) \quad (9)$$

$$\sigma = \sigma (1 - j (\tan \phi'_{12} - \tan \phi'_{11})) \quad (10)$$

where  $j$  is the imaginary notation. It is notable that the loss factors are very small (less than 10%), and therefore imaginary parts can be assumed as  $\tan \delta'_{33} \approx \delta'_{33}$ ,  $\tan \phi'_{11} \approx \phi'_{11}$ ,  $\tan \phi'_{12} \approx \phi'_{12}$  and  $\tan \theta'_{31} \approx \theta'_{31}$ , respectively.

Considering complex parameters in the electrical branch of the conventional EC, the damped capacitance in (1) is

rewritten as

$$C_d = \frac{S}{t} \left( \epsilon_{33}^T - \frac{2d_{31}^2}{s_{11}^E(1-\sigma)} \right) = C_d + \frac{1}{j\omega R_d} \quad (11)$$

where the damped capacitance  $C_d$  denotes the electrical energy storage;  $R_d$  represents the extensive dielectric loss derived in the following form,

$$\frac{1}{R_d} = \frac{\omega S}{t} \left( \epsilon_{33}^T \delta'_{33} + \frac{2d_{31}^2}{s_{11}^E(1-\sigma)^2} \cdot (\phi'_{11} - \sigma\phi'_{12} - 2\theta'_{31}(1-\sigma)) \right) \quad (12)$$

Similarly, the force factor in (2) is rewritten by complex parameters as

$$\mathbf{n} = 2\pi r \cdot \frac{d_{31}}{s_{11}^E(1-\sigma)} = n(1-j\alpha) \quad (13)$$

Here,  $\alpha$  is the phase shift derived as

$$\alpha = \theta'_{31} - \frac{\phi'_{11} - \sigma\phi'_{12}}{1-\sigma} \quad (14)$$

In the mechanical branch, the sound velocity is adjusted as

$$v_p = \sqrt{\frac{1}{\rho s_{11}^E} \cdot \frac{1}{1-\sigma^2}} = v_p(1+j\gamma) \quad (15)$$

where

$$\gamma = \frac{1+\sigma^2}{2(1-\sigma^2)}\phi'_{11} - \frac{\sigma^2}{1-\sigma^2}\phi'_{12} \quad (16)$$

The wave number  $k$  can be expressed by the sound velocity as

$$\mathbf{k} = \frac{\omega}{v_p} = k(1-j\gamma) \quad (17)$$

Further, impedances in (3) and (4) can be rewritten as

$$\mathbf{Z}_{1p} = R_{1p} + jX_{1p} \quad (18)$$

$$\mathbf{Z}_{2p} = R_{2p} + jX_{2p} \quad (19)$$

Here, the resistors  $R_{1p}$  and  $R_{2p}$  denote the mechanical losses; the reactors  $X_{1p}$  and  $X_{2p}$  represent the mechanical energy storage. It is notable that  $X_{1p}$  attributes to motional capacitor (i.e., elasticity), while the reactor  $X_{2p}$  attributes to inductor (i.e., mass). In order to clarify the physical meaning of the real and imaginary parts, the complex parameters are decoupled utilizing the properties of Bessel functions as

$$\frac{d}{d(kr)} [(kr)^n J_n(kr)] = (kr)^n J_{n-1}(kr) \quad (20)$$

$$J_{-n}(kr) = (-1)^n J_n(kr) \quad (21)$$

Therefore,

$$\frac{d}{d(kr)} [J_0(kr)] = -J_1(kr) \quad (22)$$

$$\frac{d}{d(kr)} [J_1(kr)] = J_0(kr) - \frac{1}{kr} J_1(kr) \quad (23)$$

Then, applying the Taylor expansions yields

$$\mathbf{J}_0(\mathbf{kr}) = J_0(kr) + jkr\gamma J_1(kr) \quad (24)$$

$$\mathbf{J}_1(\mathbf{kr}) = J_1(kr) - jkr\gamma [J_0(kr) - \frac{1}{kr} J_1(kr)] \quad (25)$$

In order to simplify the equations, the first order approximations are used by neglecting higher order terms with respect to small loss factors. Therefore, the resistances in (18) and (19) are derived as

$$R_{1p} = \rho v_p S_r \gamma k r \left( 1 + \frac{J_0^2(kr)}{J_1^2(kr)} \right) \quad (26)$$

$$R_{2p} = -\rho v_p S_r \cdot \frac{2\gamma(1-\sigma) + \sigma(\phi'_{12} - \phi'_{11})}{kr} \quad (27)$$

According to the derivation above, the new decoupled electromechanical EC model of the piezoelectric disk considering three types of losses turns into Figure 3.

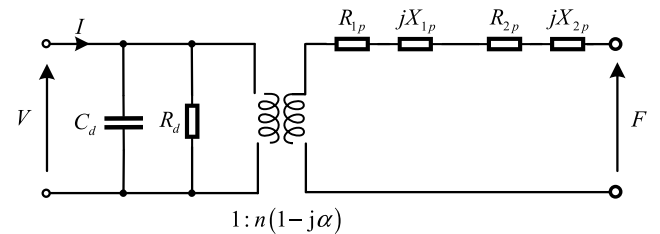


FIGURE 3. New decoupled electromechanical equivalent circuit model considering three types of losses.

### III. EXPERIMENTAL AND SIMULATION RESULTS

#### A. EXPERIMENTAL TEST AND RESULTS

Piezoelectric ceramic disks (P-42, Hongsheng Acoustic Electronic Equipment Co., Ltd., Baoding, China) are fabricated with a radius of 10 mm and a thickness of 2 mm. The impedance magnitude and phase spectra of the actual samples are measured by the Precision Impedance Analyzer (E4990A, Keysight Technologies, Inc., Santa Rosa, CA), with specifications: the maximum voltage and current are 1 Vrms and 20 mArms, the impedance measurement accuracy is 0.5%. The experimental result of impedance spectra measured on disk specimens under 500 mV applied on the thickness 2 mm is shown in Figure 4. The resonance frequency is 110.20 kHz and antiresonance frequency is 123.67 kHz of the piezoelectric disk, in the first order radial vibration mode as marked in Figure 4.

The definitions of the mechanical quality factors at resonance and antiresonance are depicted schematically in Figure 5 [21].  $Q_R$  and  $Q_A$  are utilized to denote the quality factors at the resonance and antiresonance, respectively, as

$$Q_R = \frac{f_R}{f_{R2} - f_{R1}} \quad (28)$$

$$Q_A = \frac{f_A}{f_{A2} - f_{A1}} \quad (29)$$

Here,  $f_R$  is the resonance frequency;  $f_A$  is the antiresonance frequency;  $(f_{R2} - f_{R1})$  and  $(f_{A2} - f_{A1})$  correspond to the 3dB bandwidth around the resonance and antiresonance crests in the impedance curves, respectively.

TABLE 1. Materials properties of the piezoelectric ceramic.

	Dielectric properties	Elastic properties		Piezoelectric properties	desnity
Real parameter	$\epsilon_{33}^r / \epsilon_0$	$s_{11}^E$ (m <sup>2</sup> /N)	$s_{12}^E$ (m <sup>2</sup> /N)	$d_{31}$ (C/N)	$\rho$ (kg/m <sup>3</sup> )
	1200	$12.6 \times 10^{-12}$	$-3.78 \times 10^{-12}$	$-108 \times 10^{-12}$	7600
Intensive loss	$\tan \delta_{33}^i$	$\tan \phi_{11}^i$	$\tan \phi_{12}^i$	$\tan \theta_{31}^i$	-
	0.0075	0.0021	0.0024	0.0056	-

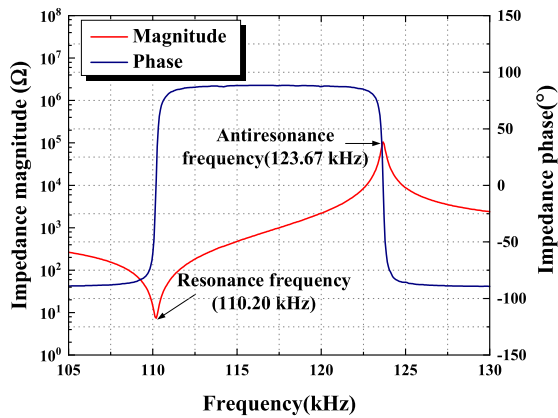


FIGURE 4. Experimental results of impedance spectra of the piezoelectric disk.

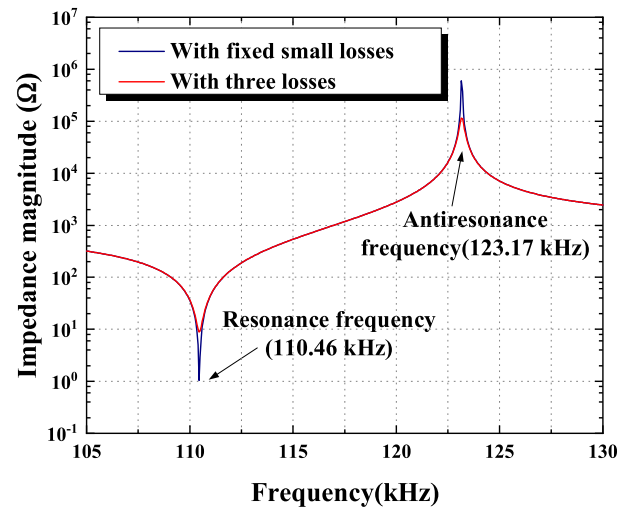


FIGURE 6. Simulation results of impedance with three losses and with fixed small losses.

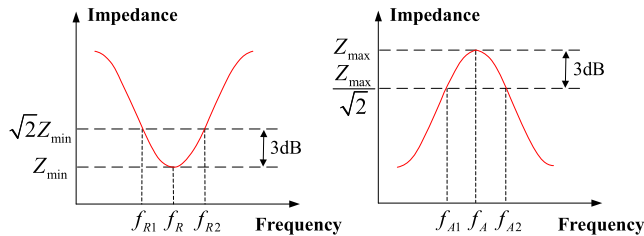


FIGURE 5. Definitions of mechanical quality factors at (a) resonance, (b) antiresonance.

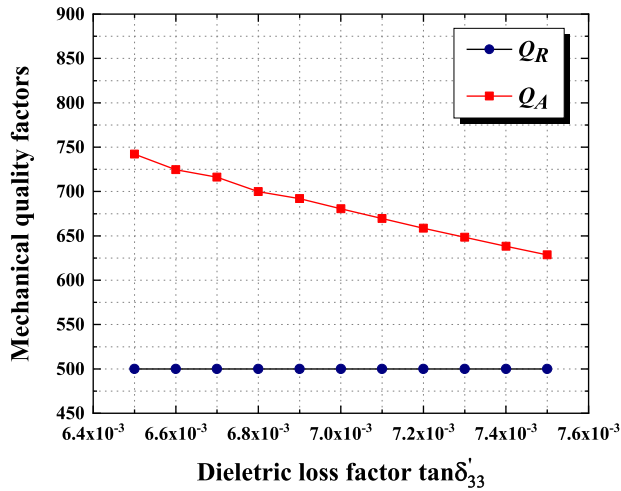
The mechanical quality factors are calculated using the 3dB bandwidth method based on three times measurement results of the impedance spectra. Experimental results of mechanical quality factors are  $485 \pm 13$  at resonance frequency and  $638 \pm 19$  at antiresonance frequency.

**B. SIMULATION RESULTS OF THE PIEZOELECTRIC DISK**

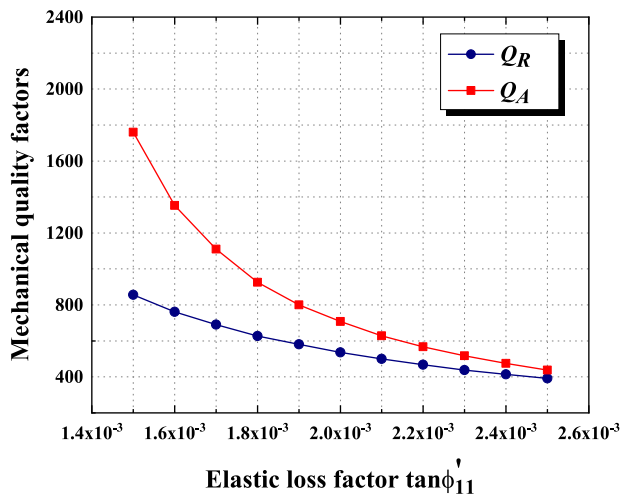
In order to verify the accuracy of the proposed EC model, the configuration of the piezoelectric disk is simulated by MATLAB (Version R2017b, The MathWorks, Inc., Natick, Massachusetts). The essential material parameters of the piezoelectric ceramic disk used for the simulation are summarized in Table 1. The real properties are measured and calculated according to the IEEE Standard [10]. The imaginary properties (i.e., intensive losses) are obtained by fitting the experimental impedance spectrum using the proposed EC model by MATLAB. It is notable that only elastic losses are related with the 3dB bandwidth at resonance frequency in impedance spectrum which could be directly determined,

while the dielectric, elastic and piezoelectric losses are all determined by 3dB bandwidth at antiresonance frequency in impedance spectrum which have to be determined after the determination of the elastic losses. When the piezoelectric disk vibrates freely, the two mechanical terminals of the proposed EC model in Figure 3 are short-circuited. Figure 6 is the comparison of the impedance spectrum simulating with considering three types of inherent losses and fixed small losses for comparison (which may be analogous to the loss-free material just to escape from the infinite divergence). The resonance and antiresonance frequencies are 110.46 kHz and 123.17 kHz in both impedance spectra. Three small losses are chosen as 0.1% of the three losses in order to demonstrate  $Q_R = Q_A$  condition. It is obvious that the resonance and antiresonance frequencies are not affected by losses. However, the 3dB bandwidth of the impedance spectra exhibits a tremendous difference for inherent losses.

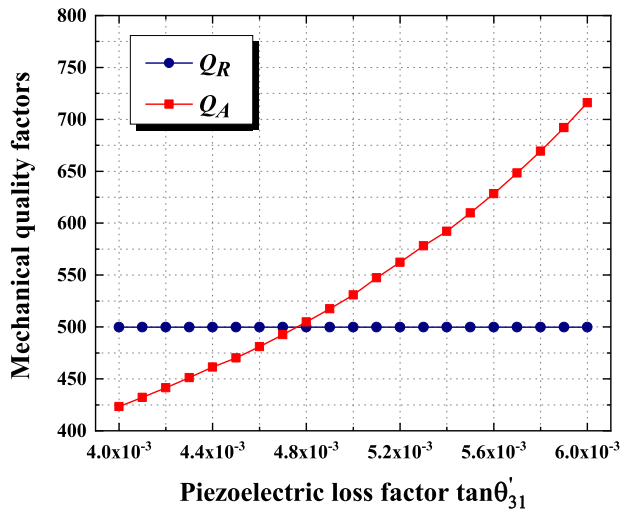
Figure 7 show simulation results of mechanical quality factors at resonance and antiresonance frequencies as functions of three types of internal losses. It is clearly seen that  $Q_R$  is not affected by dielectric and piezoelectric loss factors, while it descends slightly with the increase of elastic loss factor. At the same time,  $Q_A$  descends with the rise of dielectric and elastic loss factors, while it ascends with the increase of piezoelectric loss factor. In conclusion, the mechanical quality factor at resonance  $Q_R$  only relates with the elastic loss factor in the radial vibration mode of the piezoelectric



(a)



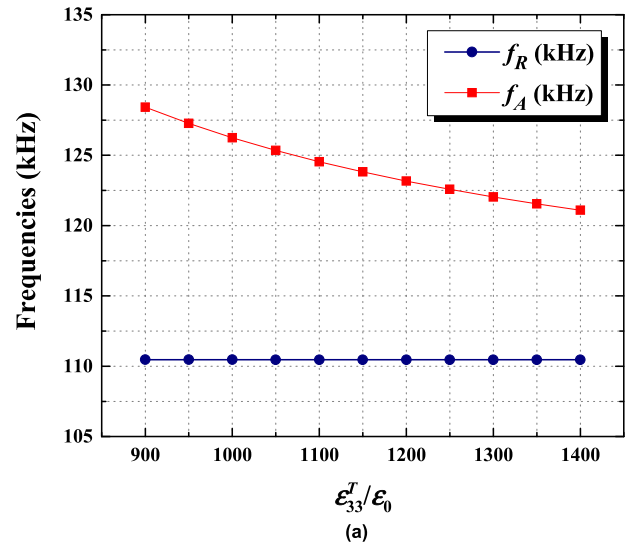
(b)



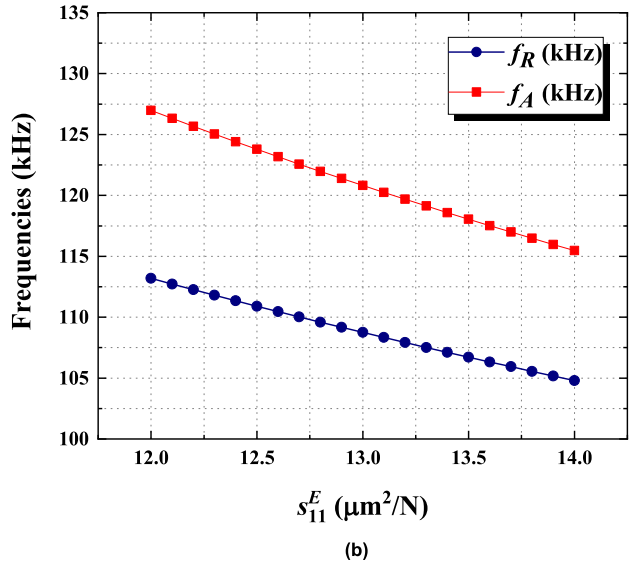
(c)

**FIGURE 7.** Simulation results of mechanical quality factors: (a)  $Q_R$  and  $Q_A$  with regard to dielectric loss factor; (b)  $Q_R$  and  $Q_A$  with regard to elastic loss factor; (c)  $Q_R$  and  $Q_A$  with regard to piezoelectric loss factor.

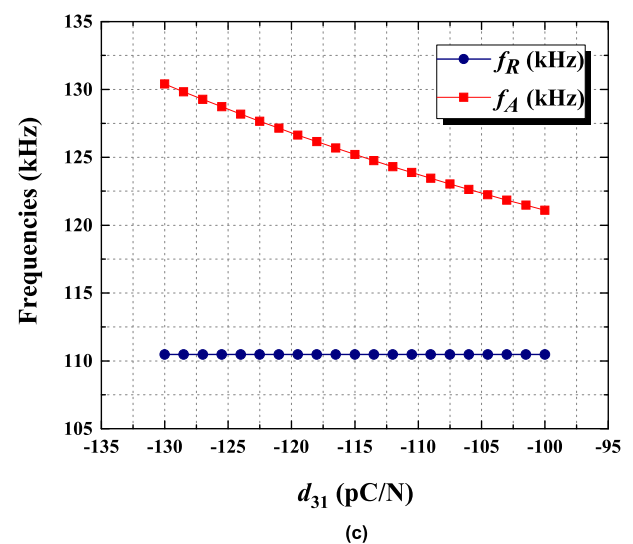
disk, while at antiresonance, the mechanical quality factor  $Q_A$  is determined by all the three loss factors. It is notable that



(a)



(b)



(c)

**FIGURE 8.** Simulation results of frequencies: (a)  $f_R$  and  $f_A$  as functions of relative permittivity; (b)  $f_R$  and  $f_A$  as functions of elastic compliance under constant electric field; (c)  $f_R$  and  $f_A$  as functions of piezoelectric constant.

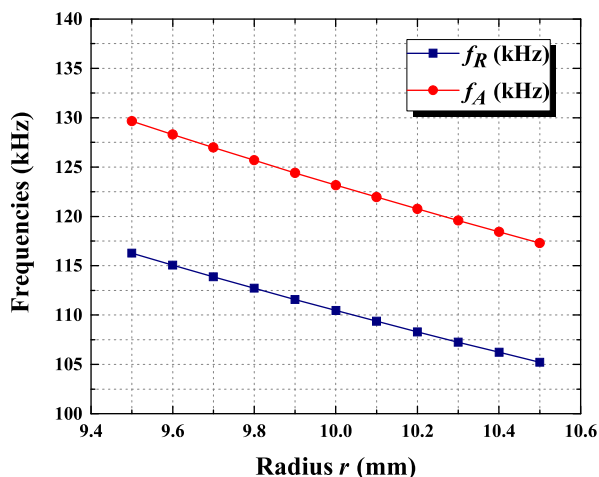


FIGURE 9. Frequencies  $f_R$  and  $f_A$  as functions of radius.

TABLE 2. Results comparison of experiment, simulation with all three losses and simulation without piezoelectric loss.

	Experiment	Three losses	Without piezo-loss
$f_R$ (kHz)	110.20	110.46	110.46
$f_A$ (kHz)	123.67	123.17	123.17
$Q_R$	485 ± 13	500	500
$Q_A$	638 ± 19	628	233

$Q_R = Q_A$  when  $\tan \theta'_{31} = (\tan \delta'_{33} + \tan \phi'_{11})/2 \approx 0.0048$  in Figure 7 (c), which corresponds to the IEEE Standard model.

In the previous research, only dielectric and/or elastic losses are considered in EC models of piezoelectric disk in radial vibration. In order to verify the critical influence of the piezoelectric loss on the heat generation of piezoelectrics, the results of experiment, simulation with all three types of losses, and simulation without piezoelectric loss are compared and summarized in Table 2. The deviation of the measured mechanical quality factors is less than 3%. It can be seen that  $Q_R > Q_A$  without including the piezoelectric loss, which is entirely contradictory to the experimental results. By contrast, simulation with three types of losses have a much better agreement with the experimental results in the columns emphasized by gray shadow, which illustrates the significance of considering piezoelectric loss in equivalent circuit to the mechanical quality factor at antiresonance frequency.

Similarly, the influence of relevant material properties on the resonance and antiresonance frequencies can be readily achieved utilizing the EC model. As shown in Figure 8, the resonance frequencies only show a downtrend with the growth of the elastic compliance, while the antiresonance frequencies decrease with the increase of relative permittivity, elastic compliance or piezoelectric constant. In addition, the relationship between the resonance or antiresonance frequencies and the structural parameters can be simulated. Here, we demonstrate the simulation results of resonance and antiresonance frequencies with regards to the radius of the piezoelectric disk by keeping the thickness  $t = 2$  mm. As shown in Figure 9, both the resonance and antiresonance frequencies decrease linearly with the increase of the radius. To sum up,

the simulation results using the EC model benefit the study of the heat generation and consequently the development of piezoelectric devices.

#### IV. CONCLUSION

In order to study the loss and heat generation in piezoelectric materials, this paper proposes a decoupled electromechanical EC model of a piezoelectric disk in radial vibration mode considering three types of internal losses. The EC model is utilized in simulation to obtain impedance spectra, and then the mechanical quality factors are calculated using the 3dB bandwidth method. A piezoelectric disk sample is fabricated and measured by experiment. Simulation results using the proposed EC model exhibit a better agreement with experimental results compared with the conventional model without piezoelectric losses, which verifies the importance of considering the piezoelectric loss for determining the mechanical quality factors (i.e., heat generation). Moreover, the proposed EC is an effective tool to study the influence of material properties and structural parameters on natural frequencies, which is beneficial for developing piezoelectric devices, such as ultrasonic motors, piezoelectric actuators, transducers and energy harvester, when utilizing a radial vibration mode of a piezoelectric disk.

#### REFERENCES

- [1] X. Zhou, W. Chen, and J. Liu, "Novel 2-DOF planar ultrasonic motor with characteristic of variable mode excitation," *IEEE Trans. Ind. Electron.*, vol. 63, no. 11, pp. 6941–6948, Nov. 2016.
- [2] Y. Liu, W. Chen, D. Shi, X. Tian, S. Shi, and D. Xu, "Development of a four-feet driving type linear piezoelectric actuator using bolt-clamped transducers," *IEEE Access*, vol. 5, pp. 27162–27171, 2017.
- [3] X. Yang, Y. Liu, W. Chen, and J. Liu, "Sandwich-type multi-degree-of-freedom ultrasonic motor with hybrid excitation," *IEEE Access*, vol. 4, pp. 905–913, 2016.
- [4] K. Uchino, "Piezoelectric ultrasonic motors: Overview," *Smart Mater. Struct.*, vol. 7, no. 3, pp. 273–285, Jun. 1998.
- [5] A. V. Mezheritsky, "Efficiency of excitation of piezoceramic transducers at antiresonance frequency," *IEEE Trans. Ultrason., Ferroelectr., Freq. Control*, vol. 49, no. 4, pp. 484–494, Apr. 2002.
- [6] H. N. Shekhani and K. Uchino, "Evaluation of the mechanical quality factor under high power conditions in piezoelectric ceramics from electrical power," *J. Eur. Ceram. Soc.*, vol. 35, no. 2, pp. 541–544, Feb. 2015.
- [7] S. Sarangapani and X. Yan, "Improvement in the electromechanical properties of a partially diced piezoelectric disc transducer," *IEEE Access*, vol. 6, pp. 70324–70330, 2018.
- [8] B. Ju, Z. Guo, Y. Liu, G. Qian, L. Xu, and G. Li, "Self-sensing vibration suppression of piezoelectric cantilever beam based on improved mirror circuit," *IEEE Access*, vol. 7, pp. 148381–148392, 2019.
- [9] K. Smyth and S.-G. Kim, "Experiment and simulation validated analytical equivalent circuit model for piezoelectric micromachined ultrasonic transducers," *IEEE Trans. Ultrason., Ferroelectr., Freq. Control*, vol. 62, no. 4, pp. 744–765, Apr. 2015.
- [10] *An American National Standard IEEE Standard on Piezoelectricity*, ANSI/IEEE Standard 176-1987, 1987, p. 74.
- [11] K. Uchino, "Introduction to piezoelectric actuators: Research misconceptions and rectifications," *Jpn. J. Appl. Phys.*, vol. 58, no. SG, Jul. 2019, Art. no. SG0803.
- [12] Y. Park, Y. Zhang, M. Majzoubi, T. Scholehwar, E. Hennig, and K. Uchino, "Improvement of the standard characterization method on k33 mode piezoelectric specimens," *Sens. Actuators A, Phys.*, vol. 312, Sep. 2020, Art. no. 112124.
- [13] H. N. Shekhani and K. Uchino, "Characterization of mechanical loss in piezoelectric materials using temperature and vibration measurements," *J. Amer. Ceram. Soc.*, vol. 97, no. 9, pp. 2810–2814, May 2014.

- [14] X. Dong, M. Majzoubi, M. Choi, Y. Ma, M. Hu, L. Jin, Z. Xu, and K. Uchino, "A new equivalent circuit for piezoelectrics with three losses and external loads," *Sens. Actuators A, Phys.*, vol. 256, pp. 77–83, Apr. 2017.
- [15] X. Dong, C. Jiang, L. Jin, Z. Xu, and Y. Yuan, "Inherent loss analysis of piezoelectrics in radial vibration and its application in ultrasonic motor," *IEEE Trans. Ultrason., Ferroelectr., Freq. Control*, vol. 67, no. 8, pp. 1632–1640, Aug. 2020.
- [16] S. Lin, "Study on a new type of radial composite piezoelectric ultrasonic transducers in radial vibration," *IEEE Trans. Ultrason., Ferroelectr., Freq. Control*, vol. 53, no. 9, pp. 1671–1678, Sep. 2006.
- [17] S. Lin, L. Xu, and H. Wenxu, "A new type of high power composite ultrasonic transducer," *J. Sound Vib.*, vol. 330, no. 7, pp. 1419–1431, Mar. 2011.
- [18] Y. Huang and W. Huang, "An improved equivalent circuit model of radial mode piezoelectric transformer," *IEEE Trans. Ultrason., Ferroelectr., Freq. Control*, vol. 58, no. 5, pp. 1069–1076, May 2011.
- [19] S. Lin, "Radial vibration of the combination of a piezoelectric ceramic disk and a circular metal ring," *Smart Mater. Struct.*, vol. 16, no. 2, pp. 469–476, Feb. 2007.
- [20] S. Lin, J. Hu, and Z. Fu, "Electromechanical characteristics of piezoelectric ceramic transformers in radial vibration composed of concentric piezoelectric ceramic disk and ring," *Smart Mater. Struct.*, vol. 22, no. 4, Mar. 2013, Art. no. 045018.
- [21] K. Uchino, Y. Zhuang, and S. O. Ural, "Loss determination methodology for a piezoelectric ceramic: New phenomenological theory and experimental proposals," *J. Adv. Dielectr.*, vol. 1, no. 1, pp. 17–31, Jan. 2011.



**CHUNRONG JIANG** was born in Fuzhou, China, in 1983. She received the B.E., M.E., and Ph.D. degrees in electrical engineering from Southeast University, China, in 2006, 2009, and 2013, respectively.

From 2011 to 2012, she worked as a Visiting Scholar with the Department of Mechanical and Aerospace Engineering, Missouri University of Science and Technology, USA. She is currently an Associate Professor of electrical engineering with the Nanjing Institute of Technology, China. Her research interest includes modeling and control of piezoelectric ultrasonic motors.



**LONG JIN** received the Ph.D. degree from the Nanjing University of Aeronautics and Astronautics, Nanjing, China, in 1997.

He has been a Professor of electrical engineering with Southeast University, since 2003. His research interests include ultrasonic motors, high power electronics technology, and robot design.



**XIAOXIAO DONG** (Member, IEEE) received the B.Sc. degree in electrical engineering from Nanjing Normal University, Nanjing, China, in 2012, and the Ph.D. degree in electrical engineering from Southeast University, Nanjing, in 2018.

From 2015 to 2016, she worked with the International Center for Actuators and Transducers, The Pennsylvania State University, as a Visiting Scholar. Since 2018, she has been a Lecturer with the College of Energy and Electrical Engineering, Hohai University, Nanjing. Her research interests include ultrasonic motor developments related to materials, theoretical modeling and control technology, piezoelectric actuators, and energy harvesting.



**ZHIKE XU** received the Ph.D. degree from Southeast University, Nanjing, China, in 2005.

He is currently an Associate Professor with the School of Electrical Engineering, Southeast University. His research interests include numerical modeling of ultrasonic motors and piezoelectric actuators.



**KENJI UCHINO** (Life Fellow, IEEE) received the M.B.A. degree, in 2008.

He has been a Founding Director of the International Center for Actuators and Transducers and a Professor of EE and MatSE with The Penn State University, since 1991. He was an Associate Director of The U.S. Office of Naval Research–Global Tokyo Office, and also the Founder and a Senior Vice President of Micromechatronics Inc., State College, PA, USA. He has authored a textbook *Entrepreneurship for Engineers*. His research interests include solid state physics, especially in ferroelectrics and piezoelectrics, including basic research on theory, materials, device designing and fabrication processes, as well as application development of solid state actuators/sensors for precision positioners, micro-robotics, ultrasonic motors, smart structures, piezoelectric transformers, and energy harvesting. He has authored 582 articles, 78 books, and 33 patents in the ceramic actuator area. He is also a Fellow of American Ceramic Society. He was a recipient of 31 awards, including IEEE-UFFC Ferroelectrics Recognition Award in 2013, and International Ceramic Award from Global Academy of Ceramics in 2016.



**YUE YUAN** (Member, IEEE) received the B.Sc. and M.Sc. degrees in electrical engineering from Xi'an Jiaotong University, Xi'an, China, in 1987 and 1990, respectively, and the Ph.D. degree from Hiroshima University, Hiroshima, Japan, in 2002.

He joined the Faculty Member of Xi'an Jiaotong University in 1990. He was with Hiroshima University from 1998 to 2002. In 2003, he joined Hohai University, Nanjing, China, as a Professor. He was the Former Dean of the College of Energy and Electrical Engineering, Hohai University. His research interests include power system operations and control, renewable energy and distributed generation, smart grid, and micro grid.

• • •